

Mid & High Latitude Nighttime Ionospheric Dynamics

GROUP 5: Experiment A
Rapid Regional (07/18/2022 22-24 LT)



ISR Summer School 2022

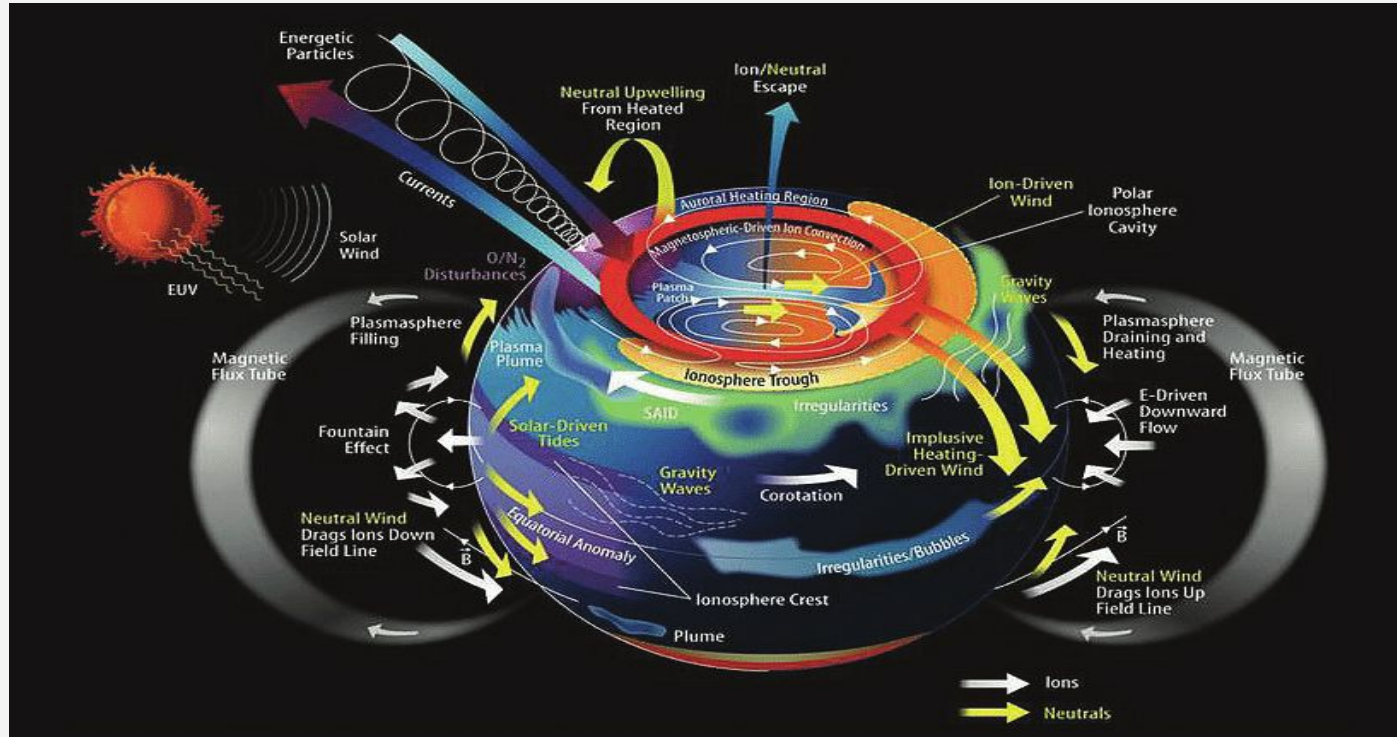
Georgia Walls, *University of Birmingham*
Nisha Yadav, *University of Scranton*
Onyinye Nwankwo, *University of Michigan*
Reynaldo Rojas, *UTEC*



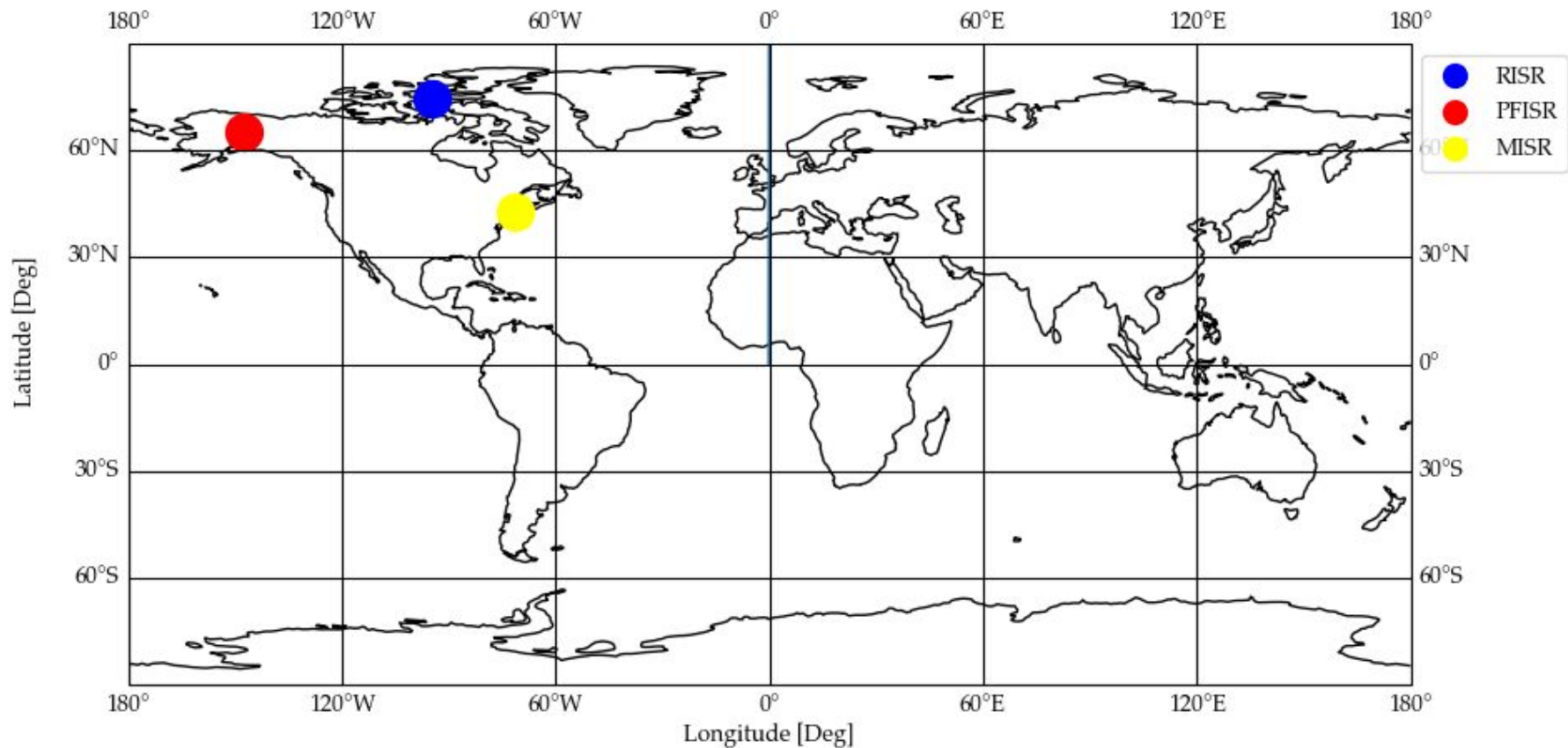
July 22nd, 2022

Experiment Objectives and Motivations

- Observe mid/high-latitude ionospheric behavior and variability during nighttime
- Observe possible geomagnetic storm (Predicted to occur between 8:00 PM 18/07/2022 to 2:00AM LT 19/07/2022)
- Use observations to analyze and compare to possible changes in the electron density

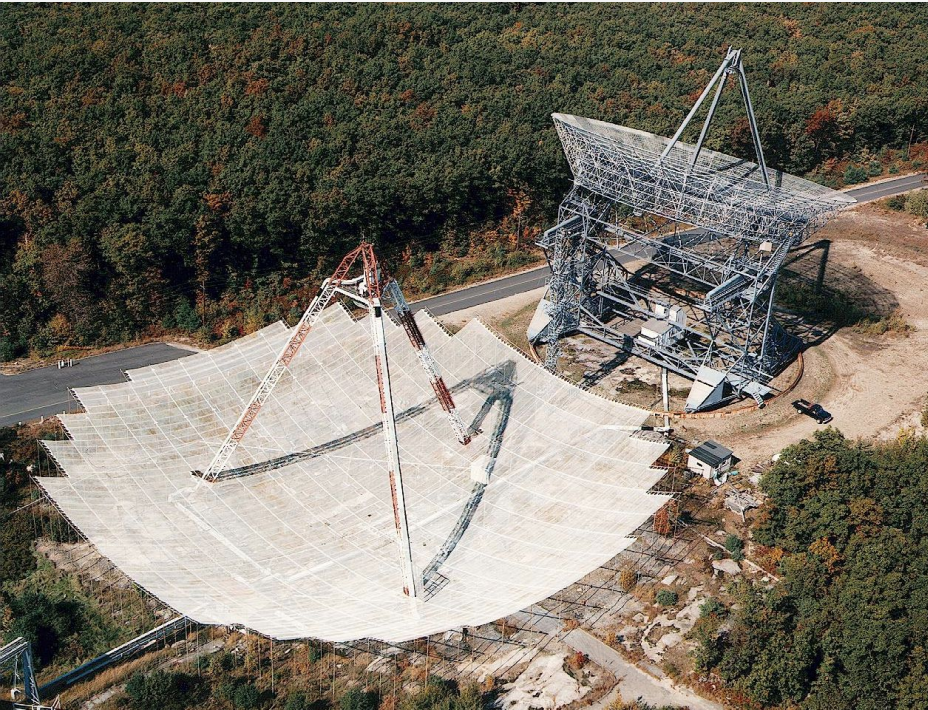


RADAR LOCATIONS



Experimental Setup (MISR)

MISR : Millstone Hill Incoherent Scatter Radar



Time: **10:00 PM to 12:00 AM LT 07/18/2022**

02:00 to 04:00 UT 07/19/2022

Characteristic : **Zenith, MISA**

Regional vectors: [**45 deg elevation, -44.98 deg azimuth**]

Wide field scans: [**6 deg elevation**]

Experiment cycle time = **~4 minutes**

- MISA fixed positions on either side of magnetic meridian
- E, F region

Experimental Setup (PFISR)

*PFISR : Poker Flat Advanced Modular
Incoherent Scatter Radar*



Location: $65^{\circ} 7'12''$ N $147^{\circ} 25'48''$ W

Geo-magnetic dip angle:
 $77^{\circ} 32'$

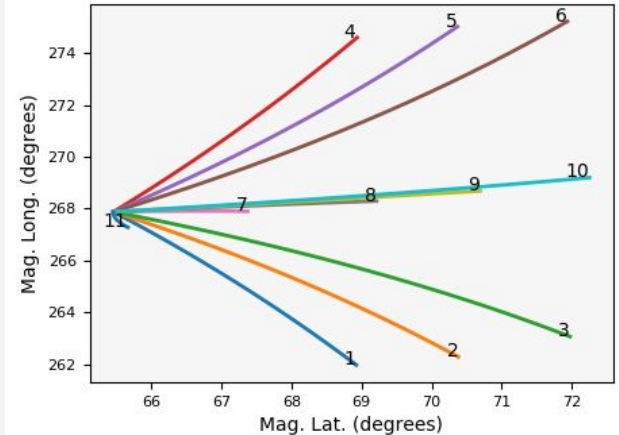
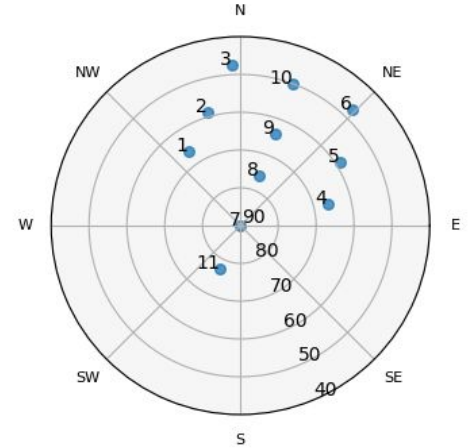
Frequency, $f = 449$ MHz

Wavelength = 0.6677 m

Bragg wavelength/2:
 0.3338 m

Antenna gain: 43 dBi

Full width half power
antenna beamwidth: 1 deg



Experimental Setup (RISR)

RISR : The Resolute Bay ISRs

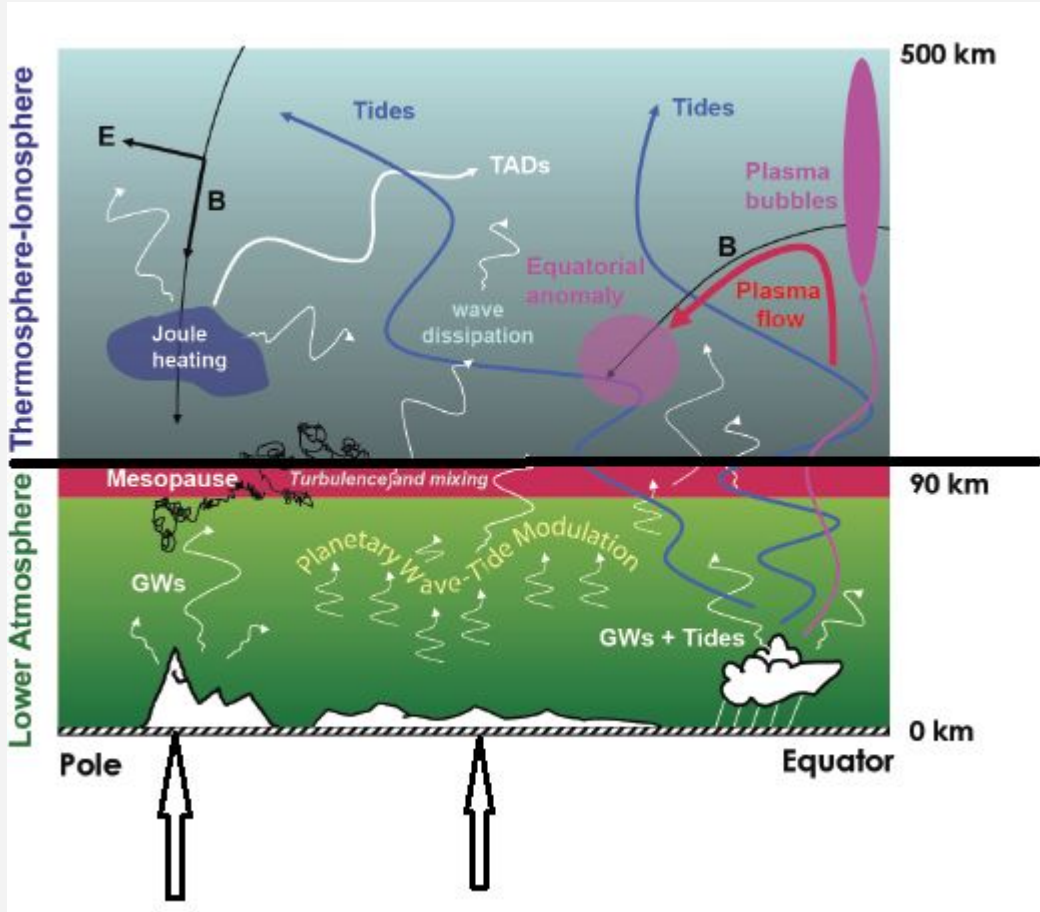
Location **74.72955° N 94.90576° W, 145 m**

Frequency Band = **430-450MHz (Nominally operates
~442.5)**

Antenna Boresight = **26° azimuth angle (E of N), 55°
elevation**

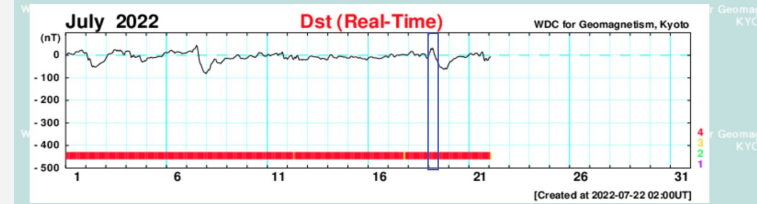
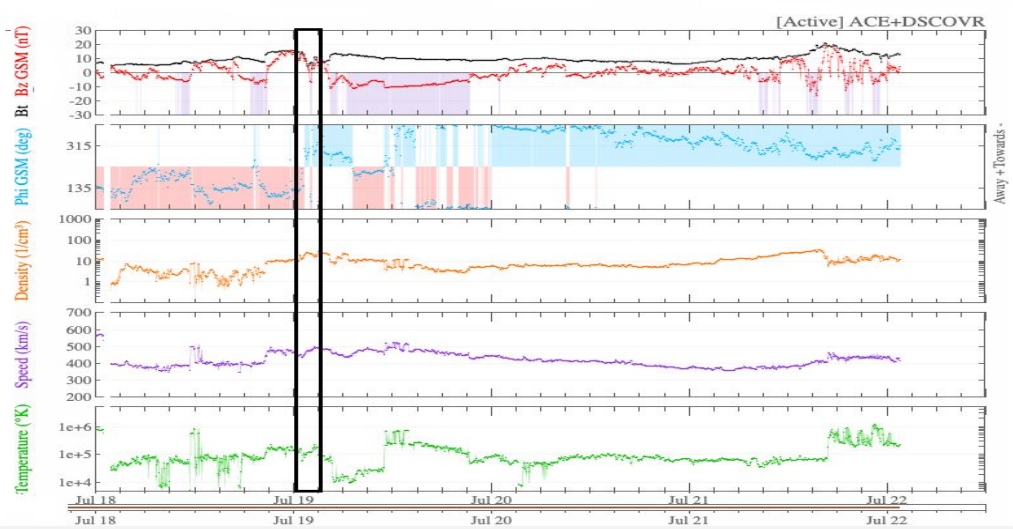


Mid & High Latitude Ionospheric Dynamics



- ❖ Location of ionospheric structures in the high latitude regions of study
- ❖ How plasma transport from high latitudes affects mid latitudes.
- ❖ The roles that magnetospheric background plays in the high latitude ionosphere.
- ❖ Mid-latitude zone is a buffer between low-latitude processes and high-latitude phenomena
- ❖ E-fields and neutral winds penetrate from high-latitudes, & equatorial plasma streams-in from events like EIA along B-field lines.
- ❖ Meridional components of the neutral wind exerts force on ionization. Geomagnetic field directs the motion of plasmas to $E \times B$ drift. Causing the lowering or raising of the altitude of F layer peak.

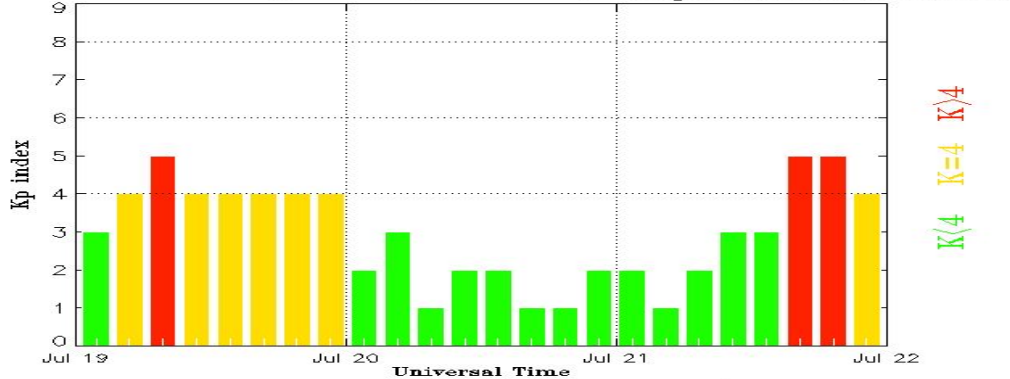
Results and Observations - *Space Weather Parameters*



WDC for Geomagnetism, Kyoto
Hourly Equatorial Dst Values (REAL-TIME)

| WDC for Geomag | WDC for Geomag JULY 2022 | | | | | | | | | | | | WDC for Geomag KYOTO | | | | UT | | | | | | | |
|----------------|--------------------------|-----|-----|-----|-----|-----|-----|-----|-----|-----|-----|-----|----------------------|-----|-----|-----|-----|-----|-----|-----|-----|-----|-----|-----|
| unit=nT | KYOTO | | | | | | | | | | | | KYOTO | | | | | | | | | | | |
| DAY | 1 | 2 | 3 | 4 | 5 | 6 | 7 | 8 | 9 | 10 | 11 | 12 | 13 | 14 | 15 | 16 | 17 | 18 | 19 | 20 | 21 | 22 | 23 | 24 |
| 1 | 2 | 5 | 10 | 9 | 7 | 7 | 5 | 3 | 4 | 3 | 10 | 14 | 16 | 15 | 14 | 16 | 21 | 20 | 23 | 20 | 14 | 10 | 8 | 12 |
| 2 | 10 | -6 | -22 | -16 | -16 | -31 | -45 | -52 | -48 | -50 | -53 | -51 | -50 | -46 | -43 | -41 | -36 | -35 | -33 | -31 | -30 | -26 | -21 | -14 |
| 3 | -7 | 1 | 5 | 7 | 7 | 7 | 9 | 11 | 20 | 24 | 24 | 22 | 19 | 23 | 19 | 18 | 23 | 19 | 17 | 9 | 3 | 3 | 14 | 18 |
| 4 | 17 | 19 | 18 | 17 | 7 | -10 | -4 | -7 | 1 | -5 | -10 | -8 | -8 | -5 | -5 | -2 | -12 | -25 | -30 | -29 | -28 | -24 | -26 | -22 |
| 5 | -15 | -12 | -12 | -13 | -10 | -9 | -11 | -12 | -10 | -10 | -10 | -9 | -8 | -5 | -5 | -6 | -5 | -6 | -4 | 2 | 8 | 11 | 11 | 11 |
| 6 | 10 | 11 | 14 | 18 | 21 | 22 | 18 | 17 | 14 | 9 | 12 | 14 | 15 | 15 | 13 | 13 | 12 | 8 | 8 | 9 | 9 | 10 | 10 | 11 |
| 7 | 13 | 16 | 17 | 18 | 18 | 16 | 14 | 26 | 27 | 29 | 36 | 44 | 32 | 8 | -20 | -36 | -41 | -52 | -62 | -71 | -76 | -77 | -82 | -77 |
| 8 | -71 | -64 | -66 | -57 | -40 | -37 | -30 | -27 | -17 | -19 | -20 | -31 | -34 | -34 | -34 | -37 | -36 | -31 | -25 | -24 | -17 | -13 | -15 | -14 |
| 9 | -13 | -15 | -15 | -16 | -15 | -15 | -12 | -8 | -7 | -2 | 1 | 2 | 0 | -5 | -12 | -15 | -14 | -14 | -16 | -17 | -15 | -14 | -12 | -12 |
| 10 | -10 | -5 | -2 | -1 | -2 | -3 | -7 | -6 | -10 | -9 | -5 | -1 | 5 | 11 | 12 | 9 | 10 | 6 | 1 | -2 | -4 | -5 | -4 | 1 |
| 11 | 4 | 2 | -2 | 0 | 2 | 3 | 4 | 7 | 7 | 9 | 5 | -1 | 4 | 7 | 6 | 7 | 15 | 3 | -15 | -14 | -10 | -13 | -18 | |
| 12 | -13 | -7 | -3 | -2 | 0 | -12 | -19 | -15 | -8 | -14 | -4 | -1 | -10 | -21 | -19 | -19 | -19 | -22 | -19 | -19 | -20 | -21 | -19 | -19 |
| 13 | -14 | -8 | -5 | -4 | -3 | -5 | -7 | -7 | -6 | -8 | -9 | -7 | -10 | -12 | -15 | -18 | -14 | -14 | -14 | -17 | -16 | -19 | -21 | -19 |
| 14 | -11 | -4 | 2 | 2 | 0 | -5 | -9 | -11 | -11 | -12 | -13 | -7 | -6 | -4 | -5 | -6 | -5 | -7 | -9 | -8 | -8 | -11 | -13 | -12 |
| 15 | -13 | -12 | -7 | -4 | -5 | -9 | -9 | -8 | -7 | -8 | -9 | -12 | -13 | -10 | -12 | -14 | -15 | -16 | -16 | -17 | -16 | -21 | -20 | -14 |
| 16 | -11 | -9 | -7 | -8 | -8 | -11 | -12 | -12 | -12 | -12 | -14 | -14 | -15 | -15 | -14 | -14 | -11 | -9 | -8 | -6 | -3 | -4 | -8 | -10 |
| 17 | -5 | 1 | 4 | 5 | 3 | -1 | -7 | -7 | -3 | 0 | 1 | 0 | 0 | 1 | 2 | 3 | 4 | 3 | 3 | 3 | 1 | 1 | 1 | 4 |
| 18 | 8 | 11 | 16 | 16 | 11 | 3 | -1 | 3 | 4 | 3 | 3 | -5 | -3 | 2 | 5 | 7 | 6 | 5 | 4 | -7 | -14 | -14 | -2 | |
| 19 | 9 | 16 | 30 | 25 | 31 | 19 | 4 | -5 | -18 | -19 | -30 | -40 | -50 | -53 | -53 | -56 | -59 | -62 | -61 | -57 | -61 | -59 | -40 | -40 |
| 20 | -33 | -27 | -28 | -24 | -20 | -16 | -15 | -14 | -12 | -9 | -6 | -6 | -6 | -5 | -6 | -8 | -6 | -6 | -10 | -10 | -9 | -6 | -3 | 0 |

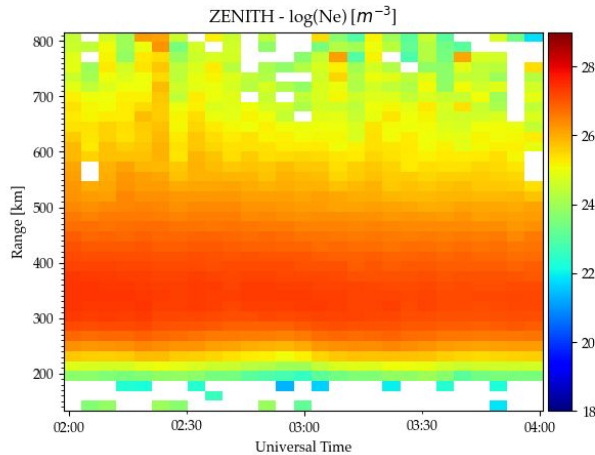
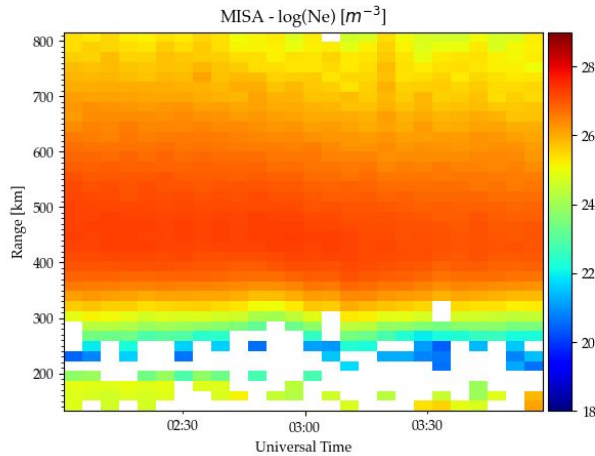
Estimated Planetary K index (3 hour data) Begin: 2022 Jul 19 0000 UTC



- Bz turn southward at 01:55 UT
- Kp index was approximately 3
- Solar wind speed increased to around 500 km/s
- Dst index was above 10 nT

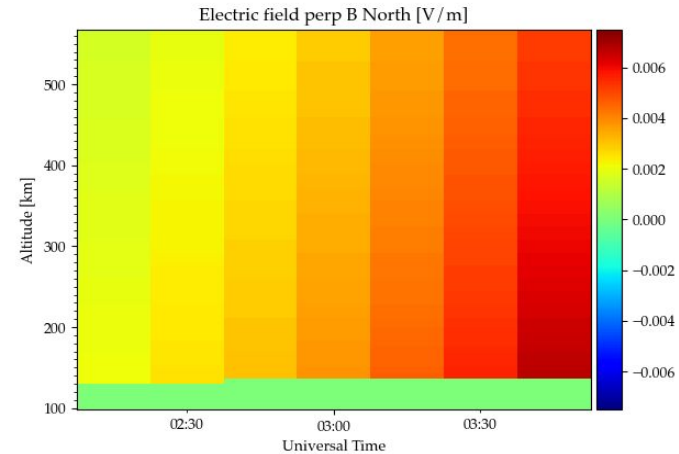
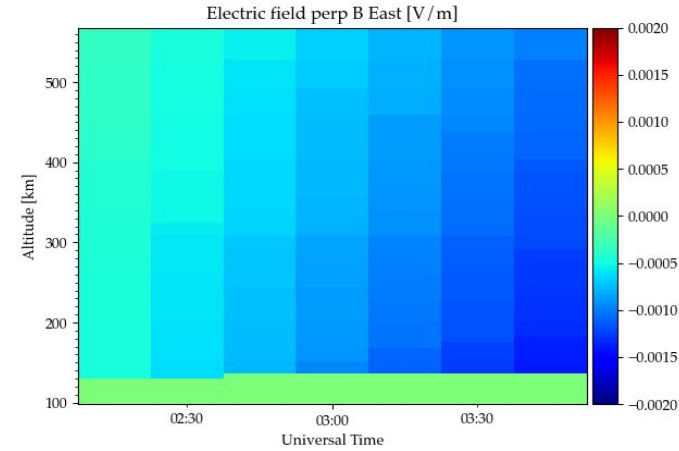
The southward IMF Bz leads to negative incursion of Dst index when the solar wind speed exceeds 600 km/s. Kyung-Eun Choi et al., (2017)

Results and Observations - *Nighttime Electron Densities*

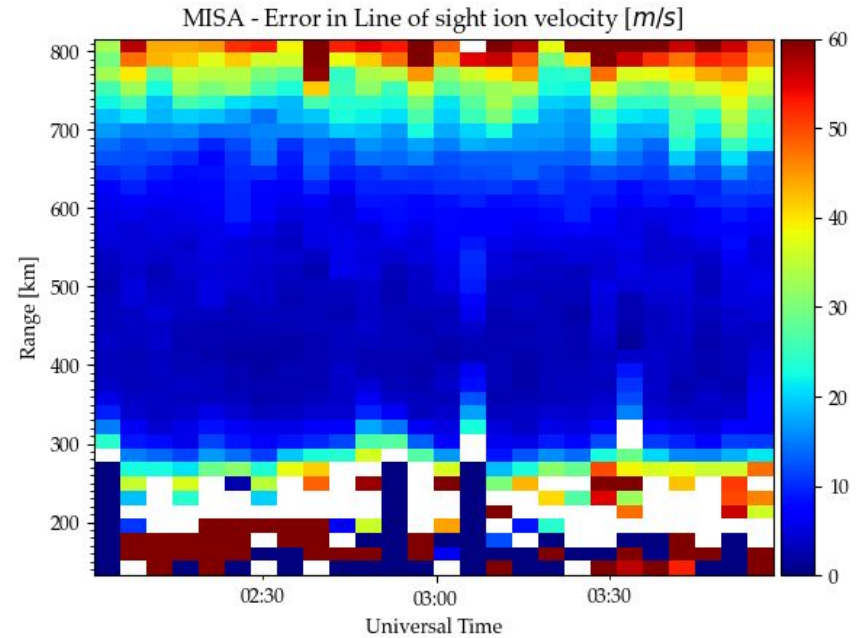
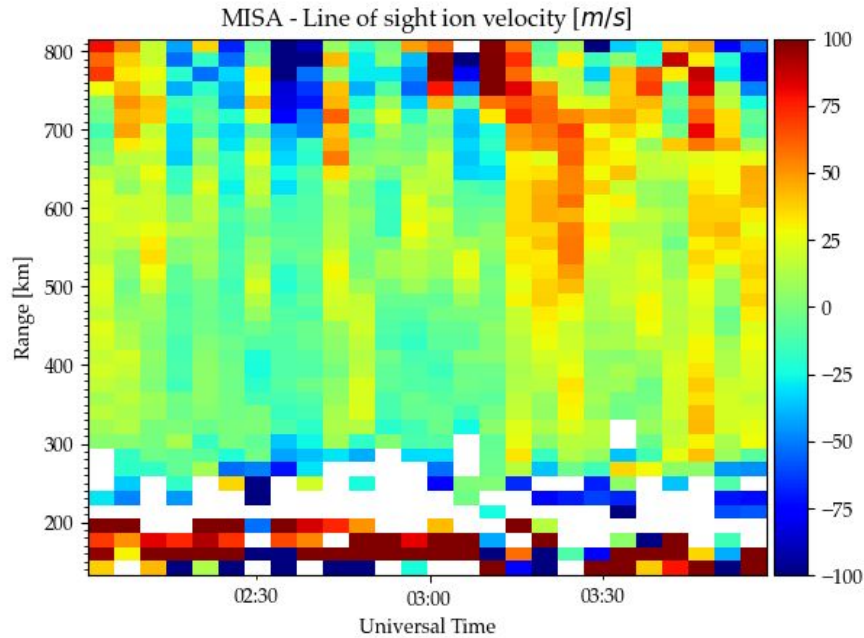


- Electron density increased upto the F layer peak, resulting in increase in nighttime F layer height.
- East/North electric field was decreasing/increasing spatially and temporally.

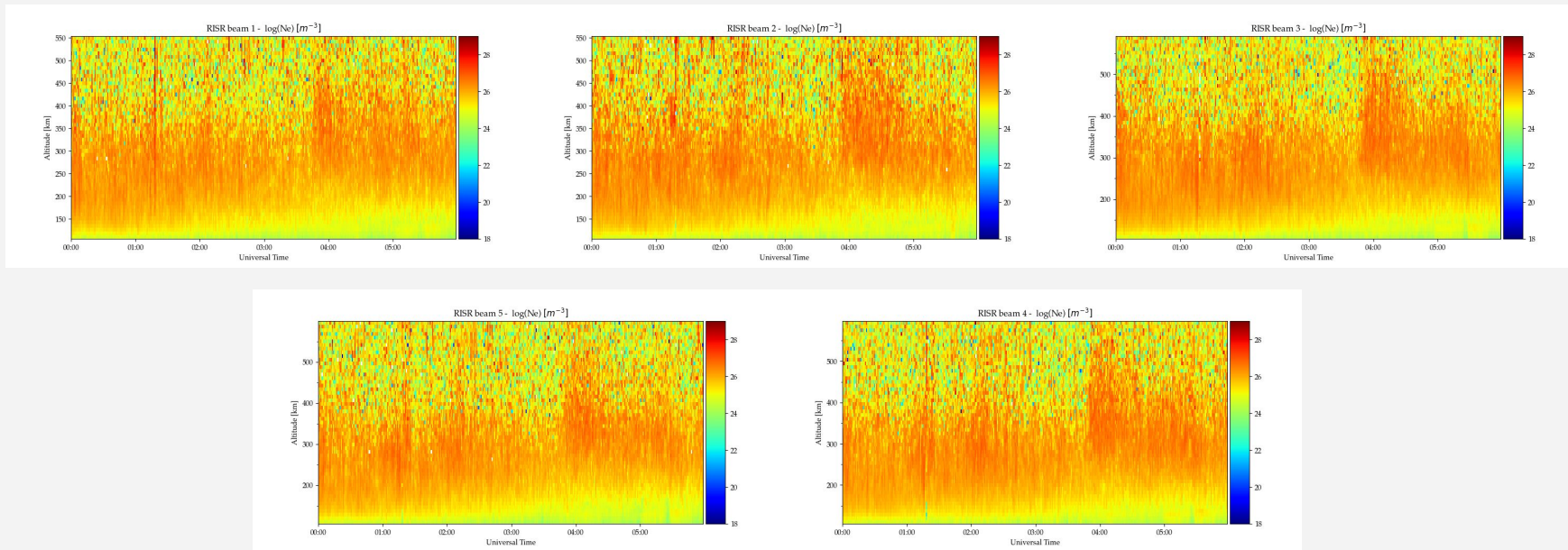
- At the nightside of the solar terminator, the Earth's ionosphere crosses into the dark side of the Earth.
- The E region conductivity decays as the E layer disappears causing the enhancement of the Northward electric field.
- The increase in Northward electric field creates a corresponding enhanced eastward electric field and upward drift of plasma.



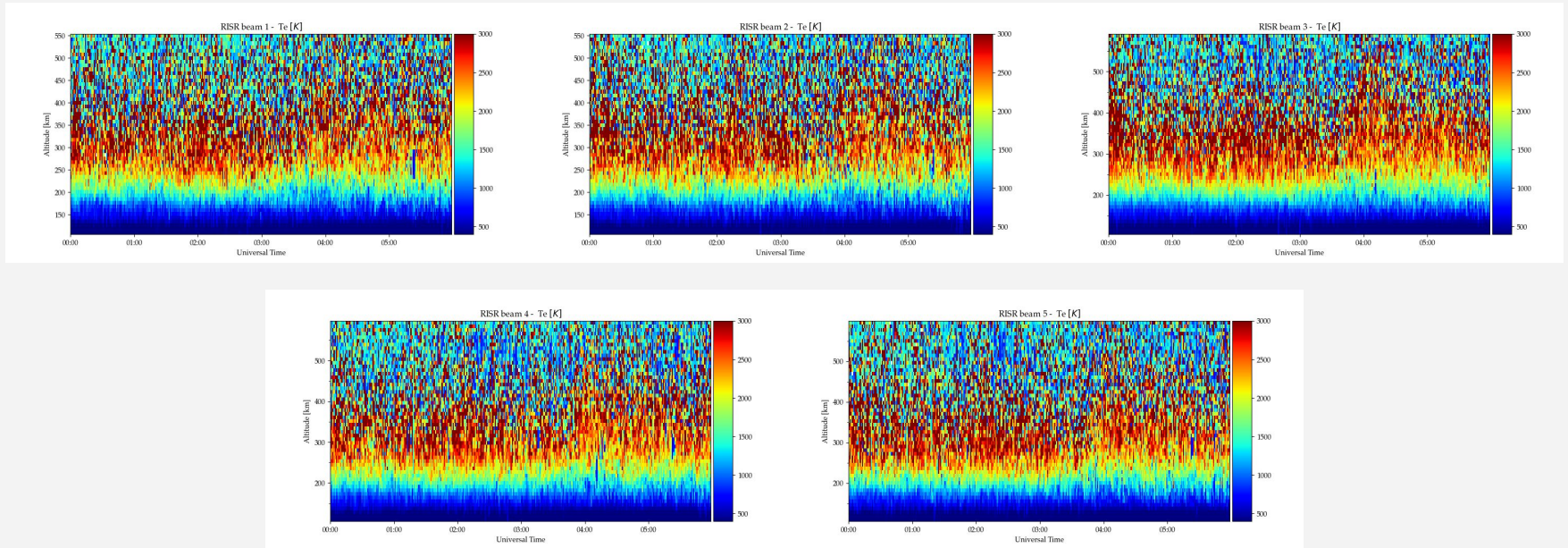
Results and Observations - *Ion behaviour*



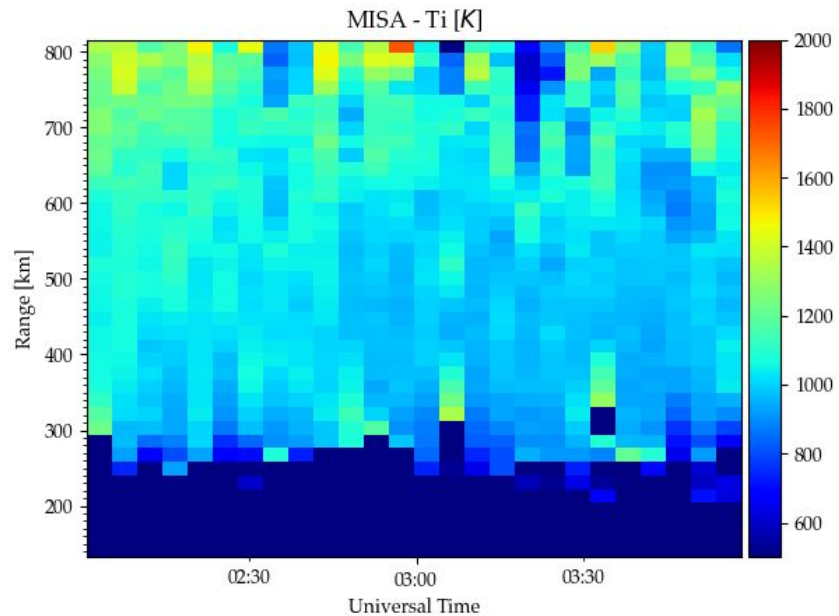
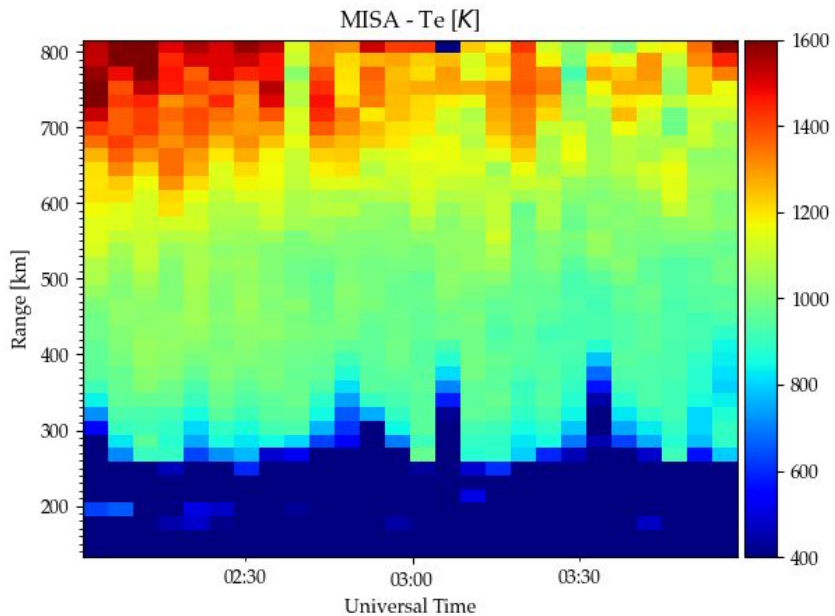
Results and Observations - *Nighttime Electron Densities for RISR*



Results and Observations - *Nighttime Electron Temperatures for RISR*

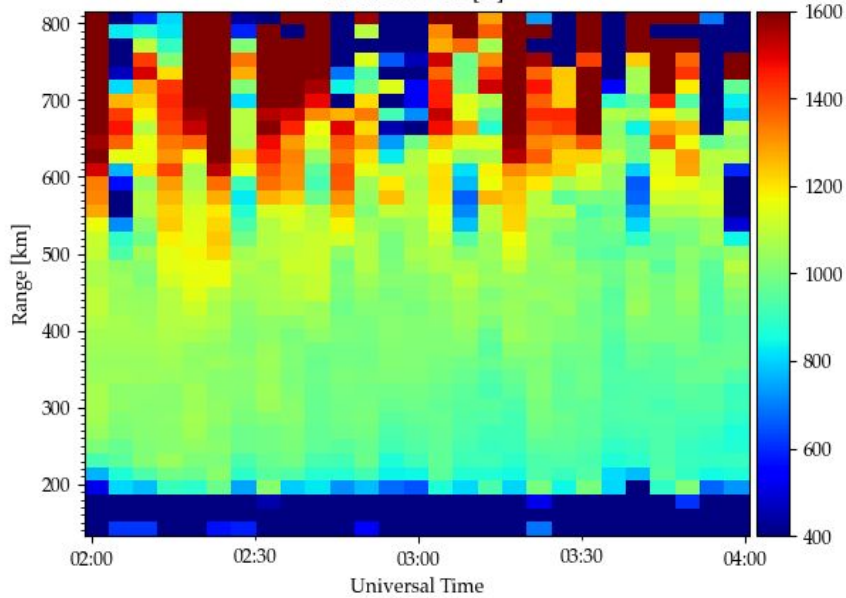


Results and Observations - T_e & T_i variation

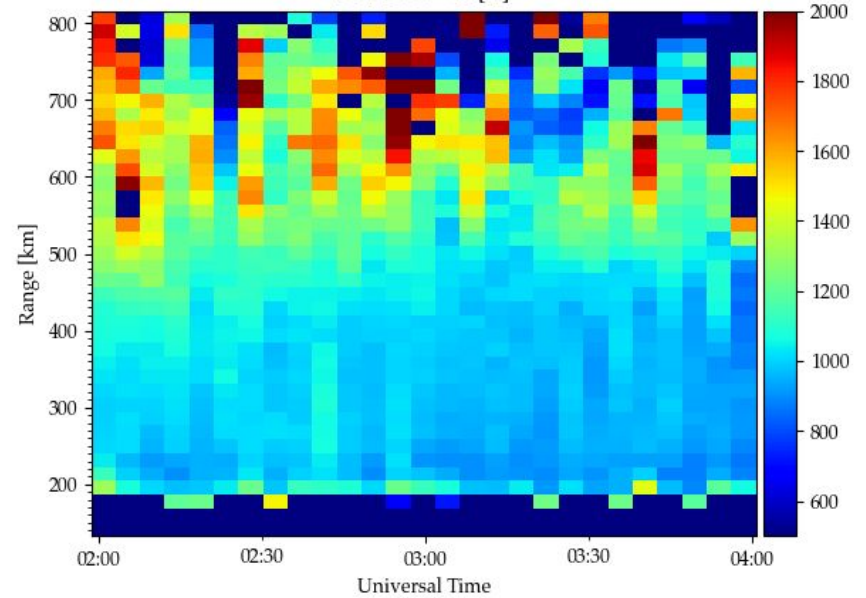


Results and Observations - T_e & T_i variation

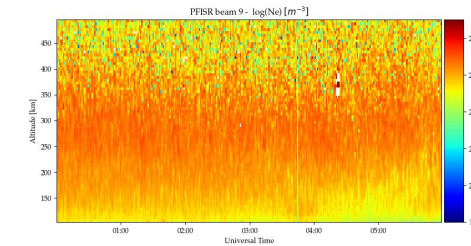
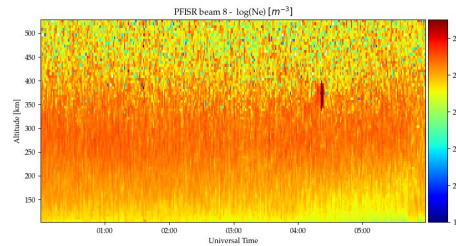
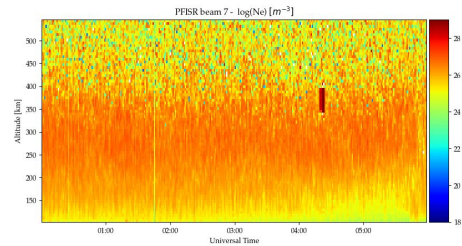
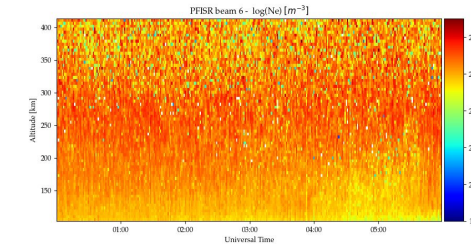
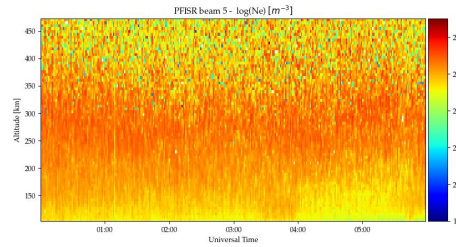
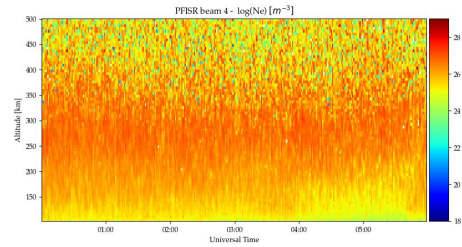
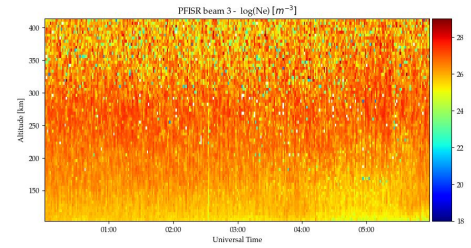
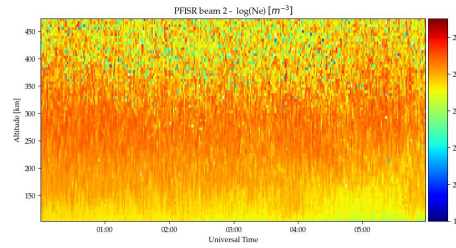
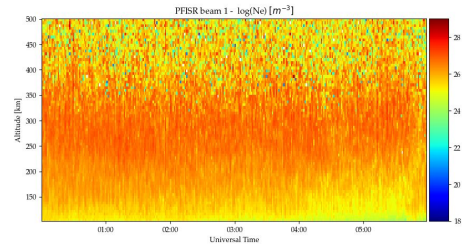
ZENITH - T_e [K]



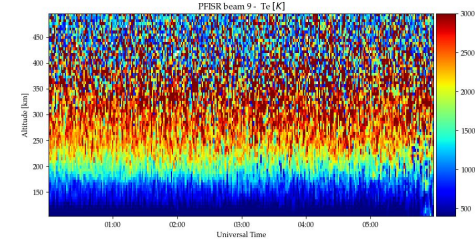
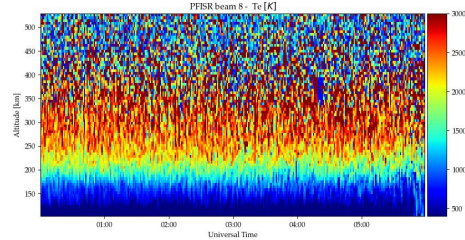
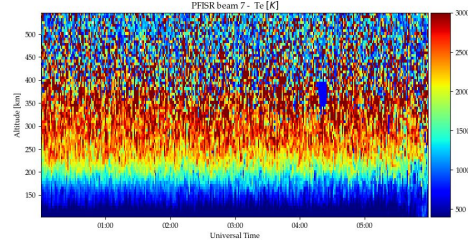
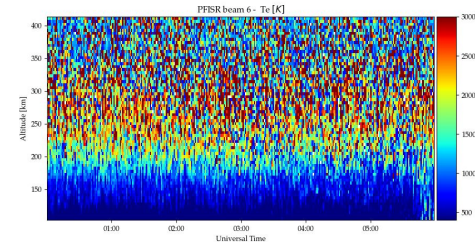
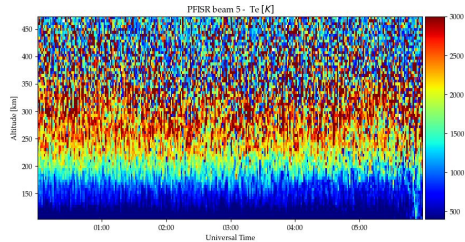
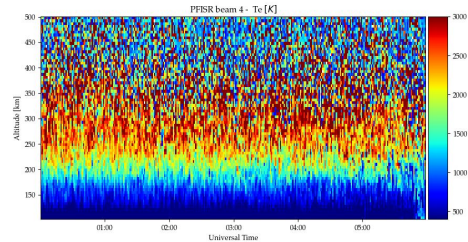
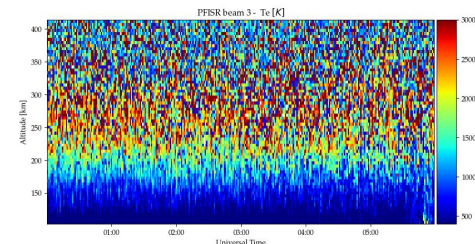
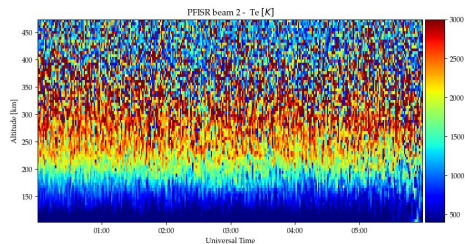
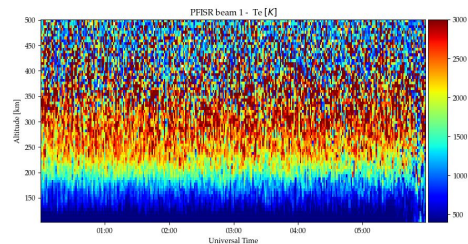
ZENITH - T_i [K]



Results and Observations - *Nighttime Electron Densities for PFISR*



Results and Observations - *Nighttime Electron Temperatures for PFISR*



Conclusions

- Moderate geomagnetic conditions
- Electron density peak disagreed with decrease in E-field enhancement - winds??)
- Doppler velocity plots demonstrated plasma drift both away and toward the radar, which may relate to spikes in electron density
- Small peak in Te and decrease in Ti right before peaks in electron density

Suggestions for Future Work

- Integrate neutral winds/HWM for comparison with electron density
- Make a comparison with stormtime conditions

Thank You!



